A

Heatmap of RNA-seq from Invitro FL cells, pre-transplantation in mice. LogFC 1 and FDR ≤ 0.05

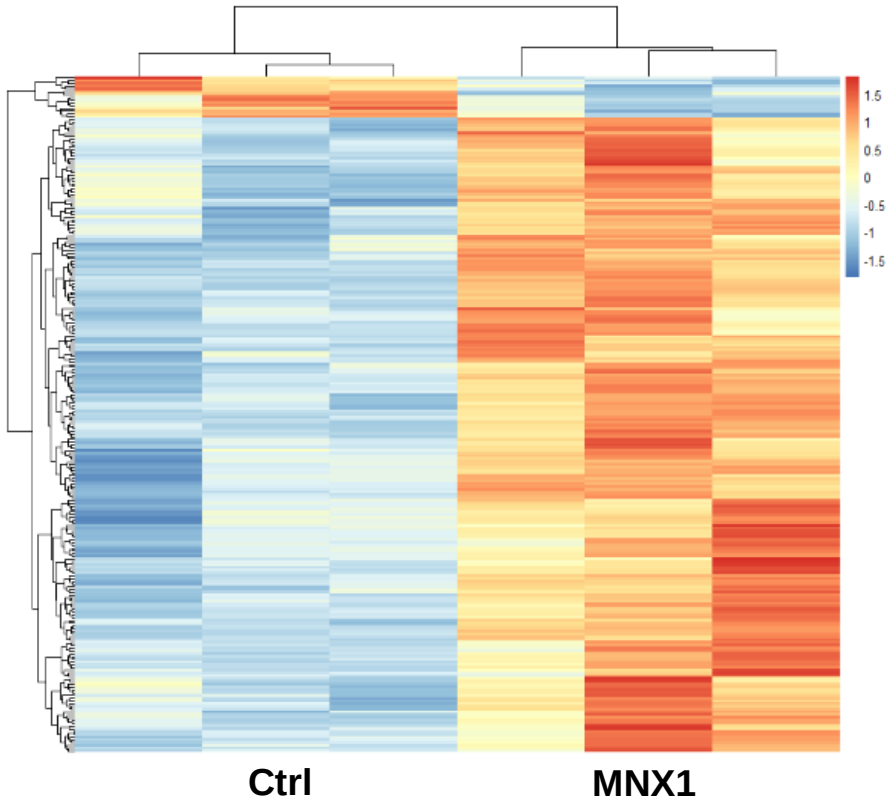

B

Volcano plot of RNA-seq from Invitro FL cells, pre-transplantation in mice. LogFC 1 and FDR ≤ 0.05

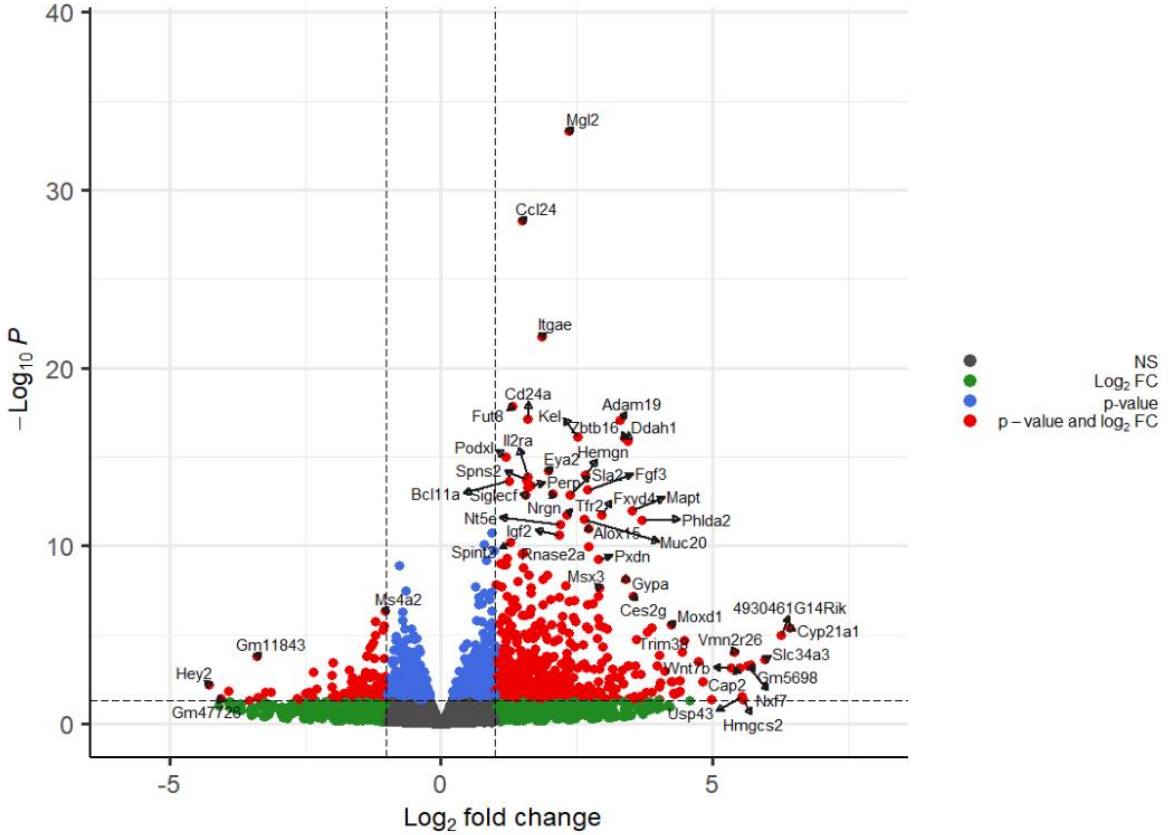

Supplementary figure 1

A

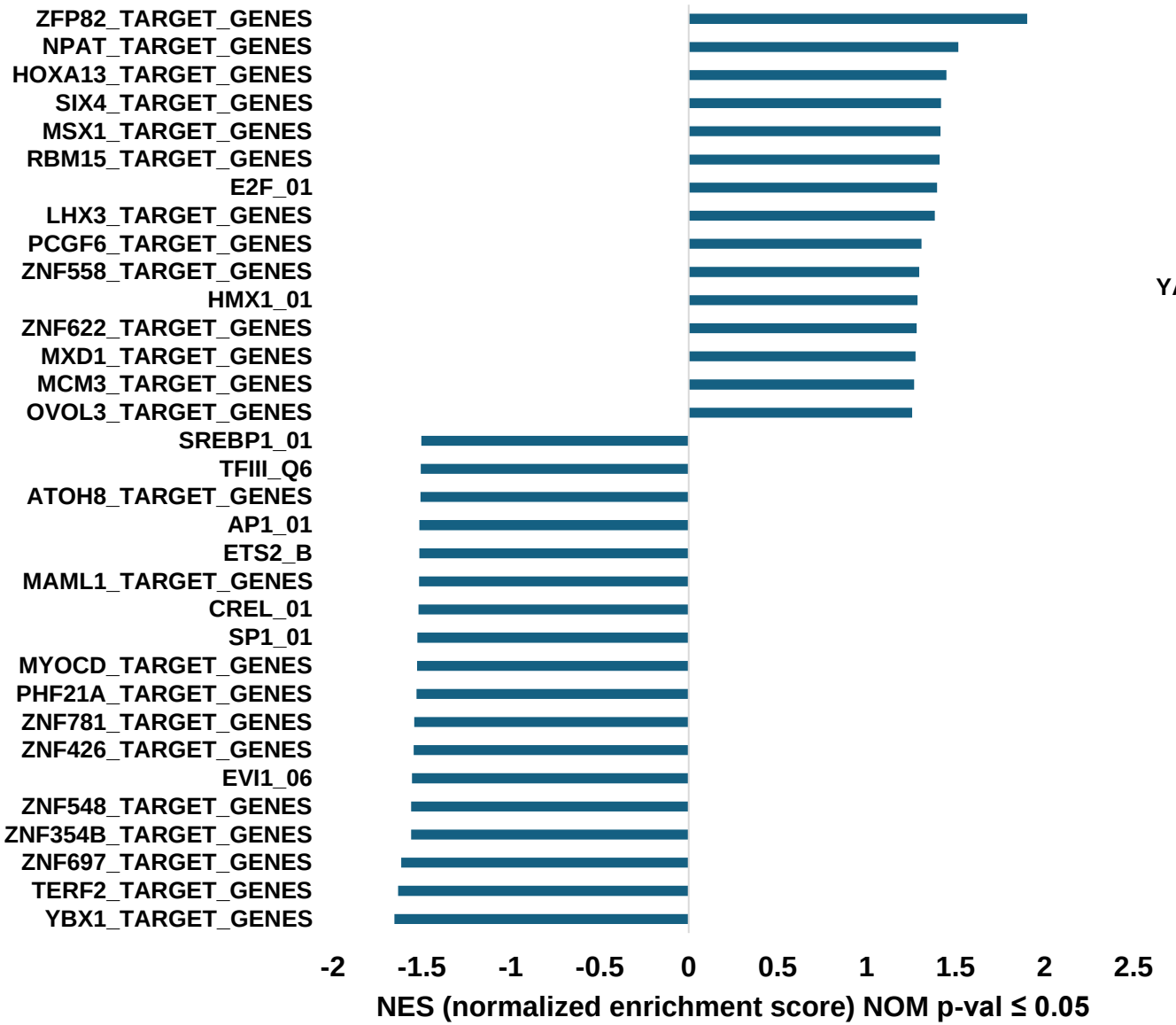

B

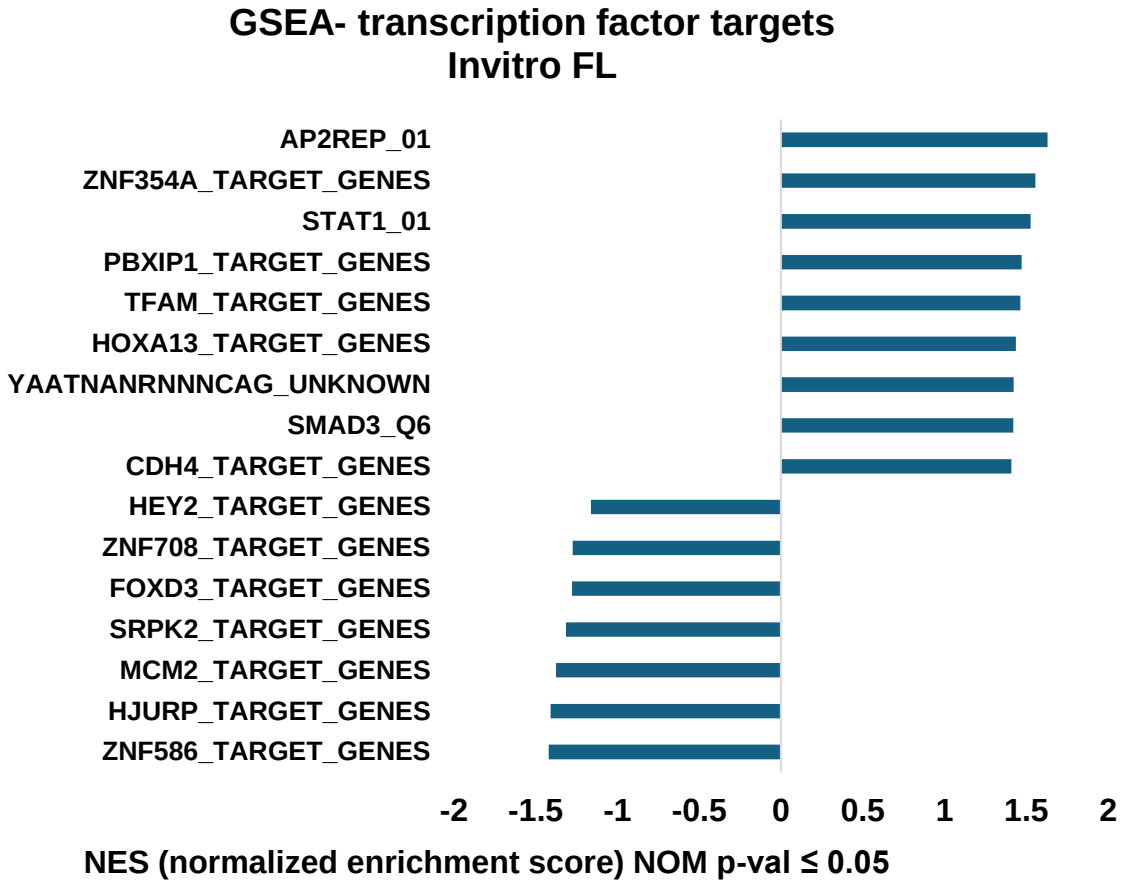

Supplementary figure 2

A

Invivo BM from NSG mice

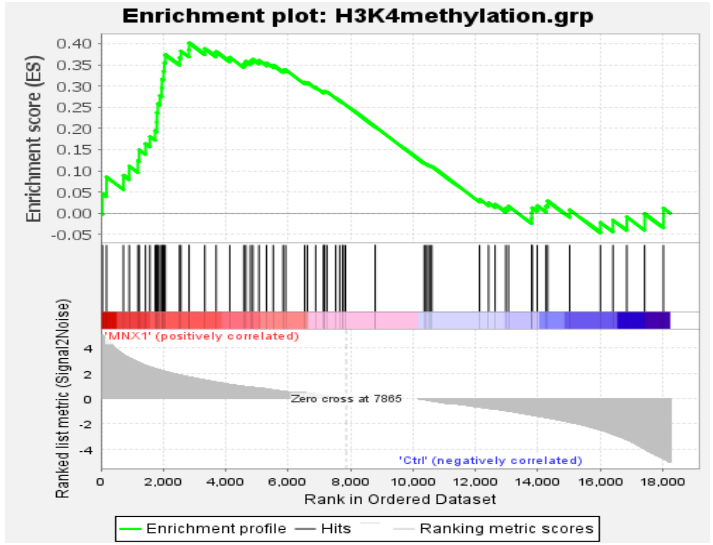

Invitro FL cells, pre-transplantation in mice

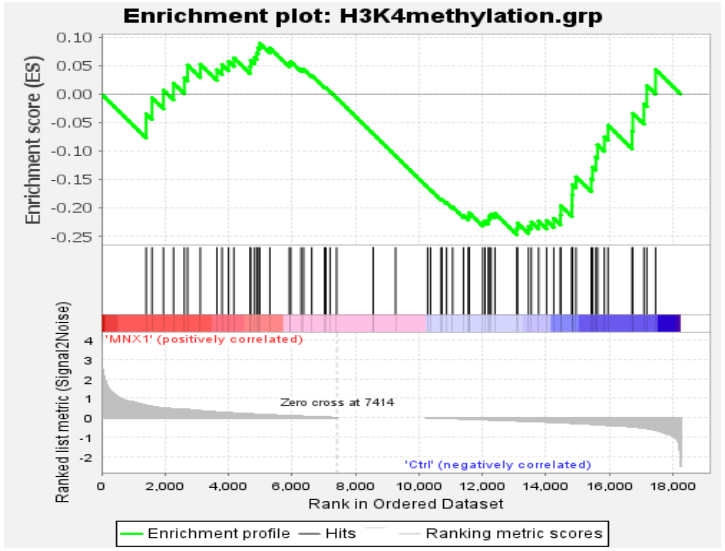

B

Invitro FL cells

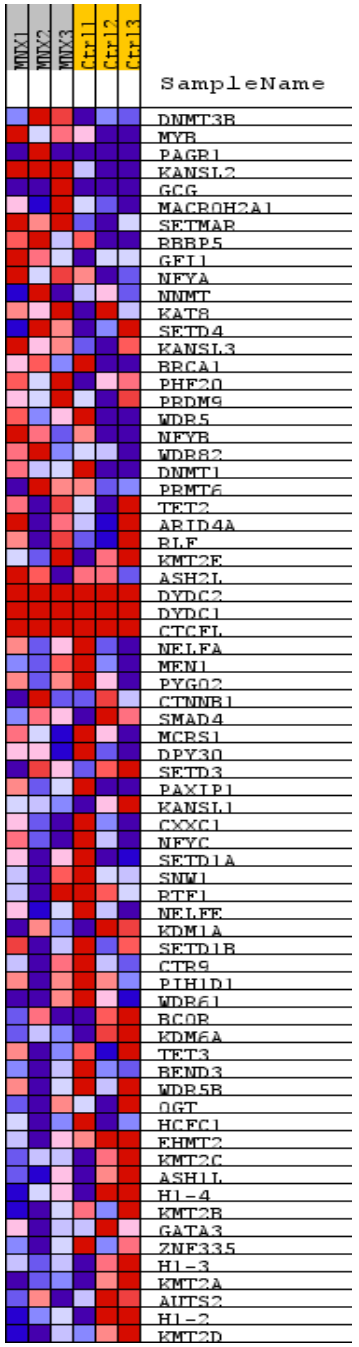

Invivo BM from NSG mice

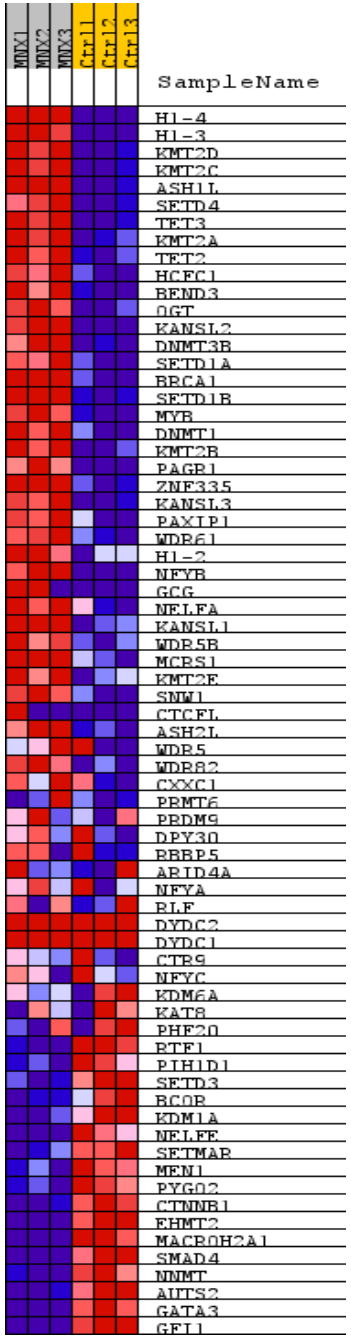

Supplementary figure 3

A

H3K4me3 (ACT-Seq)
leukemia BM cells

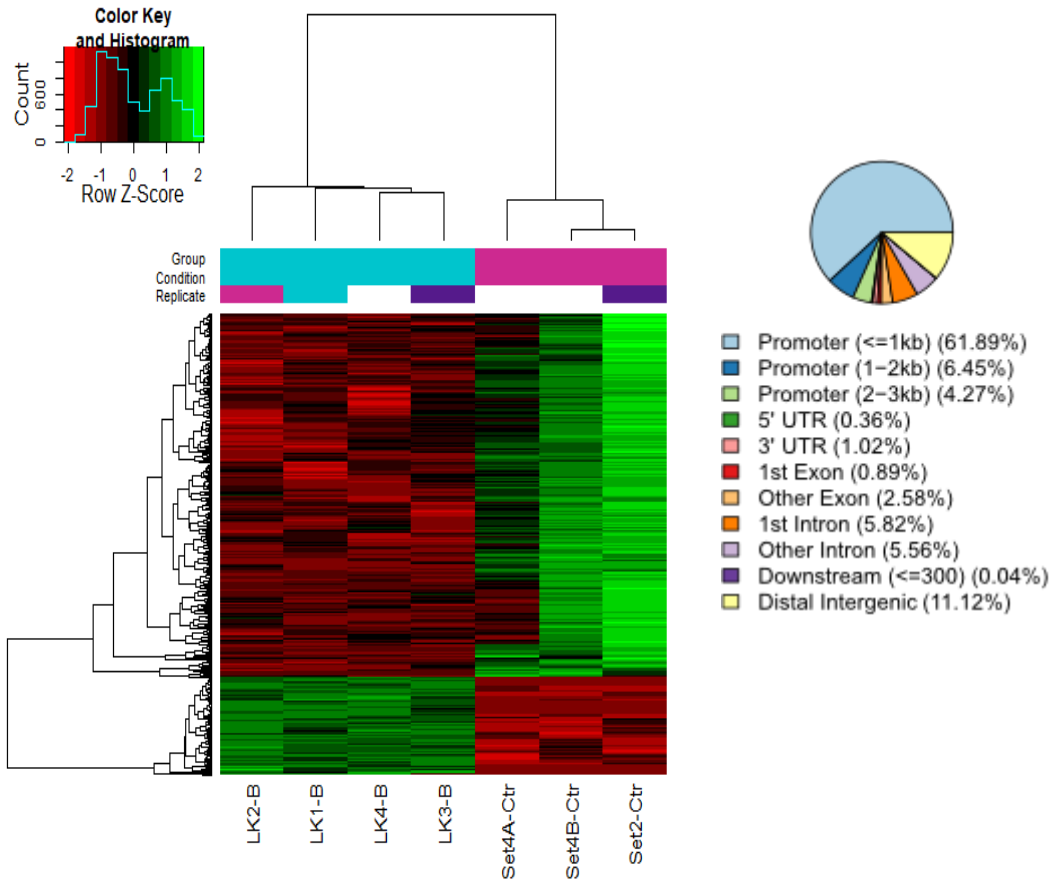

B

H3K4me1 (ACT-Seq)
leukemia BM cells

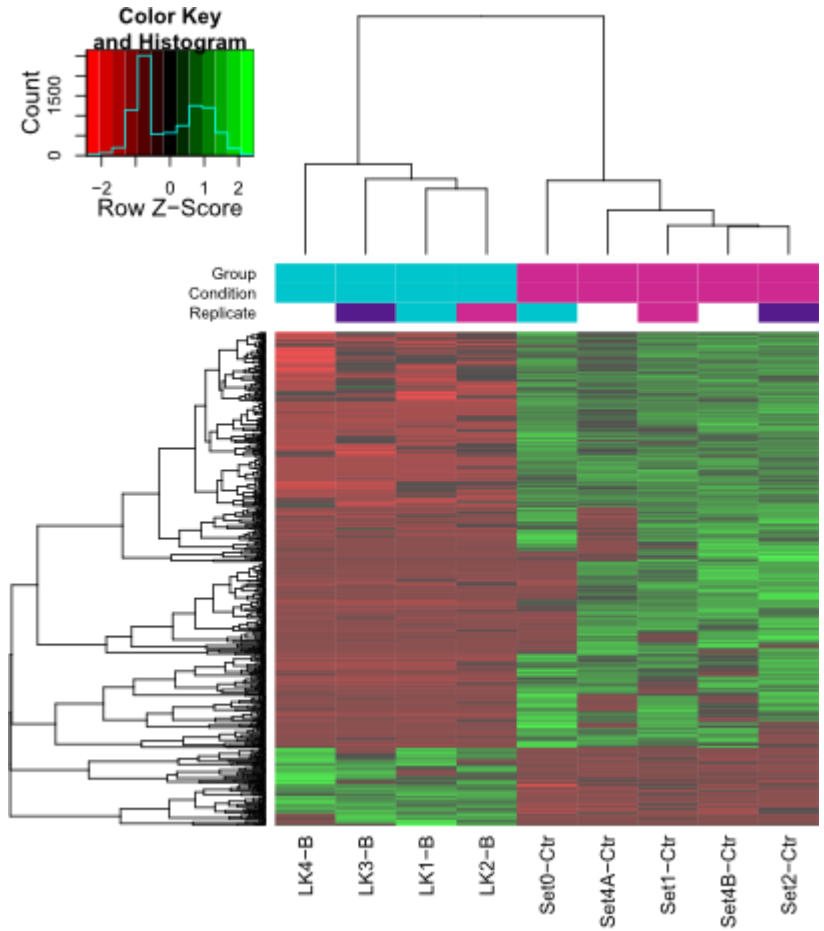

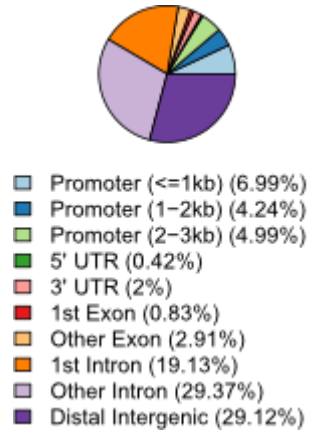

Supplementary figure 4

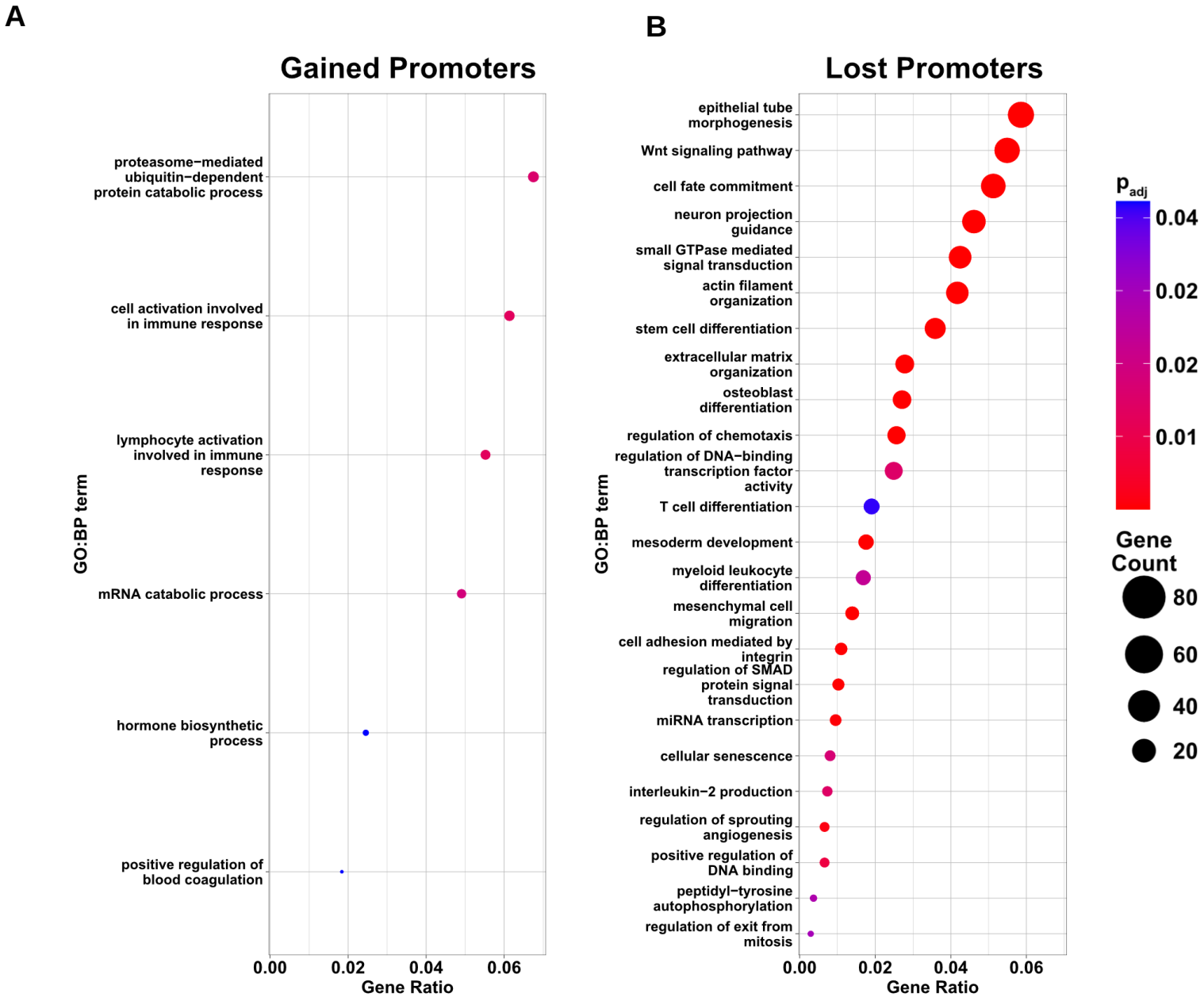

Supplementary figure 5

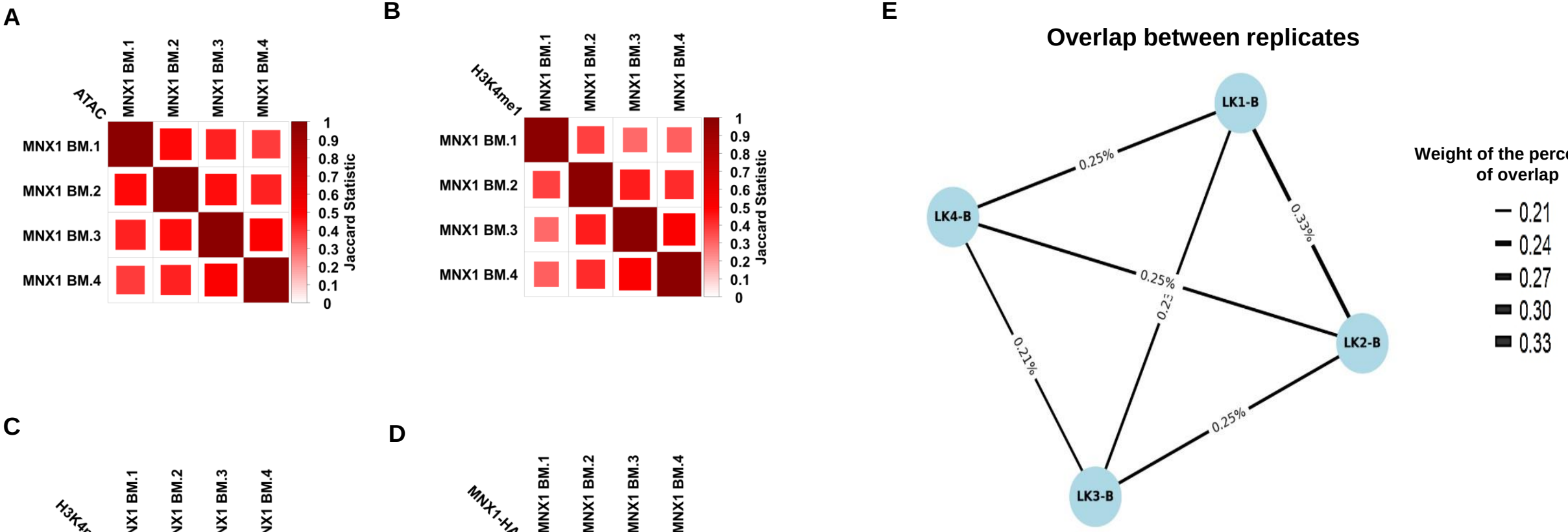

Supplementary figure 6

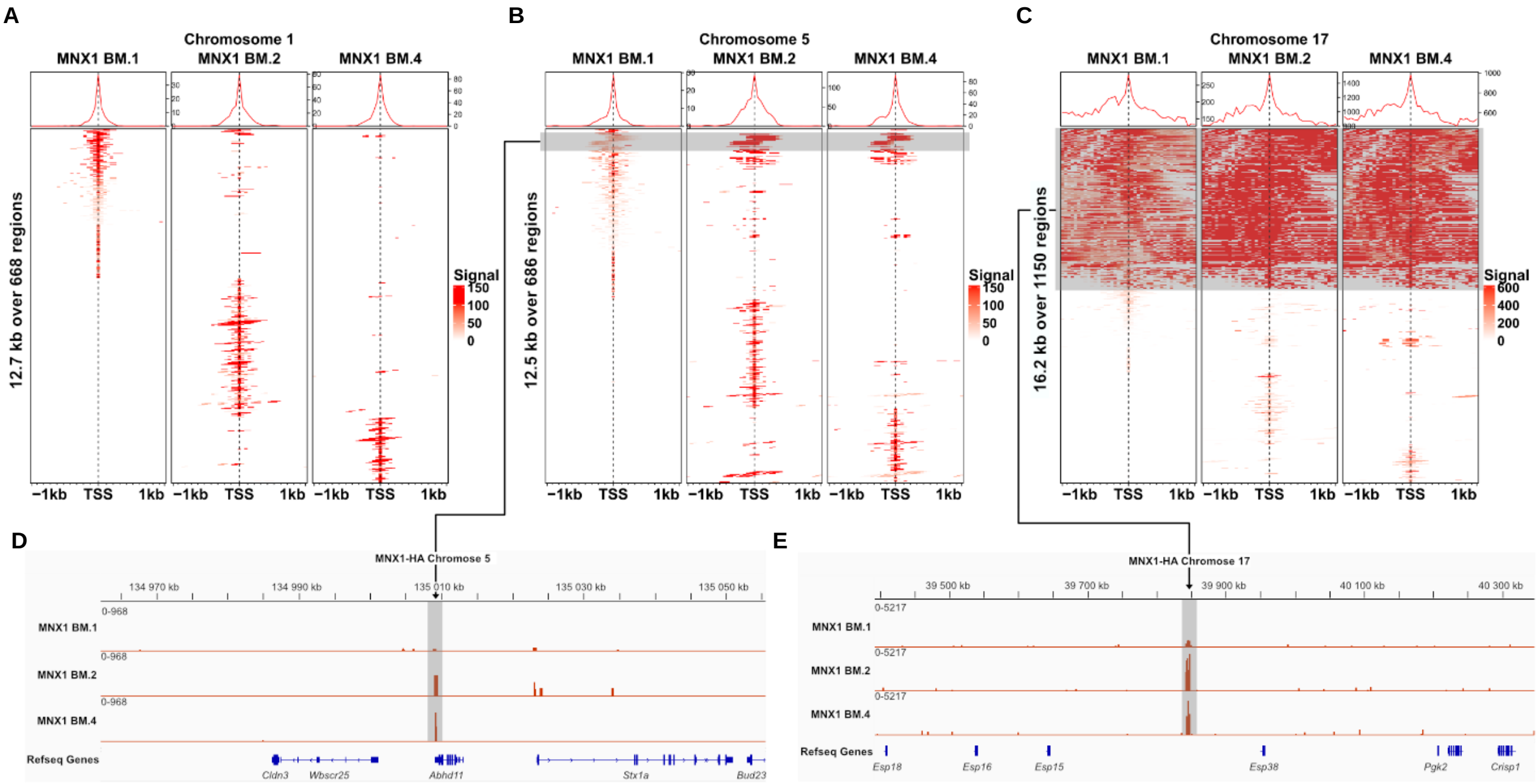

Supplementary figure 7

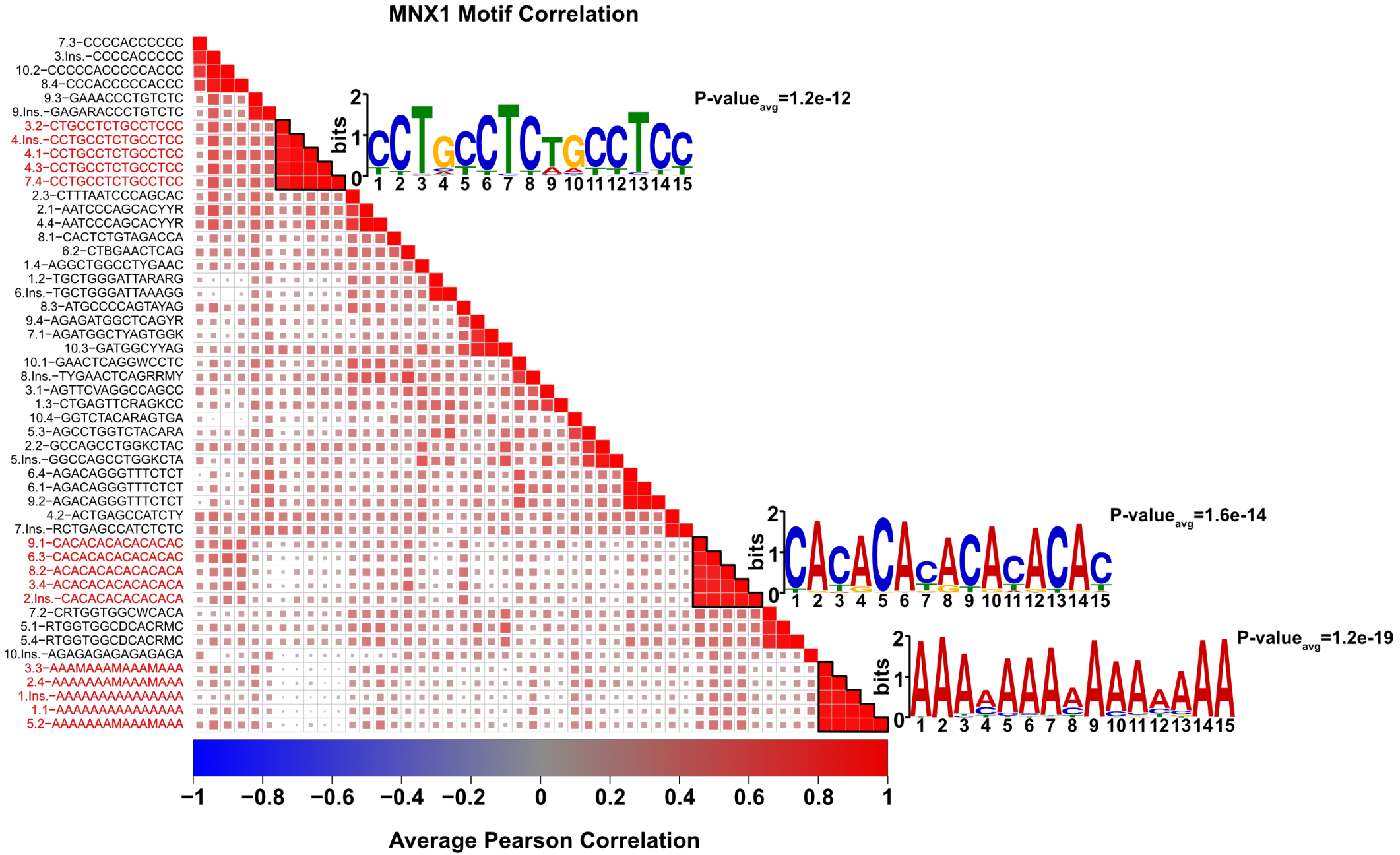

Supplementary figure 8

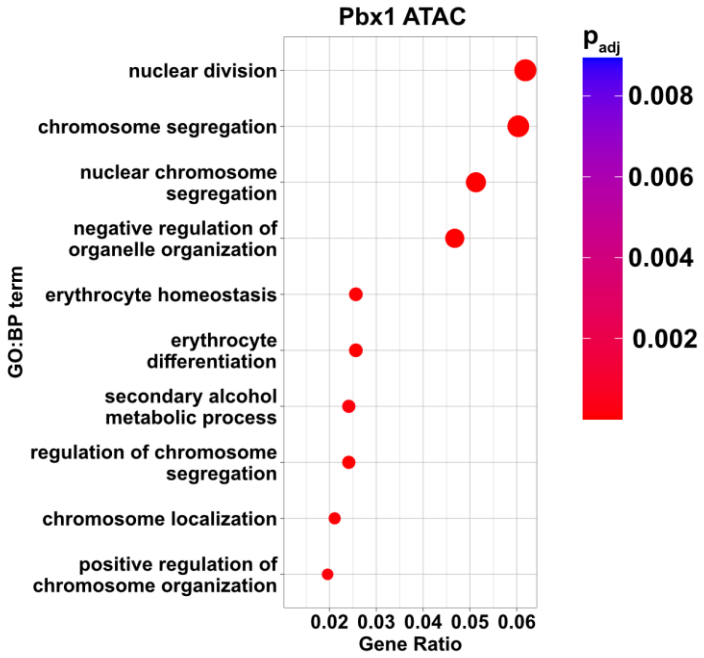

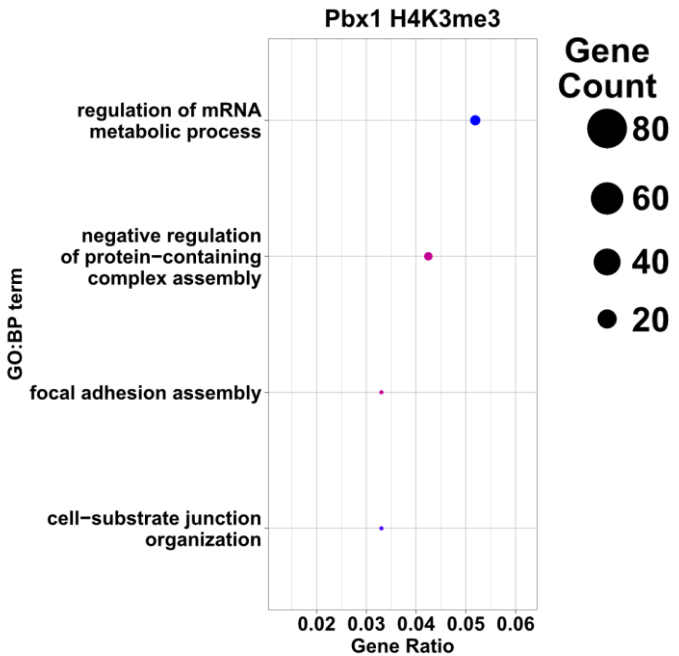

Supplementary figure 9

Supplementary figure legends

Supplementary Figure 1. Differential gene expression resulting from MNX1 ectopic expression in *in vitro* fetal liver cells compared to cells transfected with an empty vector. (A) Log fold change heat map of downregulated (blue) and upregulated (red) differentially expressed genes of leukemia BM cells with MNX1 ectopic expression (MNX) in comparison with FL cells with empty vector (Ctrl). **(B)** Volcano plot depicting gene differential expression analysis of MNX1-vector transduced *in vitro* FL cells relative to empty vector transduced FL cells, (red) genes that are differentially expressed according to the cut-off criteria of a p-value<0.05 (log-transformed in the figure) and log2 fold change > |1|, (green) genes not differentially expressed only achieving log2 fold change > |1|, (blue) genes not differentially expressed only achieving a p-value<0.05, (gray) genes not differentially expressed.

Supplementary Figure 2. Transcription factors responsible for MNX1-driven gene expression. (A-B) Barplot of normalized enrichment score (NES) for significant gene sets as determined by GSEA using the TF legacy gene set collections and the differentially expressed genes in **(A)** mice leukemia BM cells. **(B)** pre-transplantation invitro FL cells transduced with MNX1.

Supplementary Figure 3. Alterations in histone methylation associates with leukemia development. (A) GSEA enrichment plot for H3K4methylation in (upper) leukemia BM cells relative to *in vitro* FL cells and (lower) FL cells transduced with MNX1 vector relative to FL cells transduced with empty vector. **(B)** Heatmap depicting expression of H3K4methylation gene set in (left) FL cells transduced with MNX1 vector and (right) leukemia BM cells.

Supplementary Figure 4. Annotation and Heatmap Analysis of H3K4me3 and H3K4me. (A) Heatmap of regions with differentially increased (green) and decreased (red) binding of H3K4me3 in mice leukemia BM cells (LK) relative to FL cells transduced with empty vector (Set-Ctr), as well as a corresponding pie chart displays the annotation of these regions. **(B)** Heatmap of regions with differentially increased (green) and decreased (red) binding of H3K4me1 in mice leukemia BM cells (LK) relative to FL cells transduced with empty vector (Set-Ctr) as well as a a corresponding pie chart displays the annotation of these regions. Regions with a log fold-change (logFC) ≥ |1| and false discovery rate (FDR) of ≤0.05 were considered differentially bound.

Supplementary Figure 5. Pathway enrichment analysis of promoter regions with differential H3K4me3 binding in leukemia mice BM overexpressing MNX. Bubble plot illustrating the pathway enrichment analysis for increased H3K4me3 binding to promoters **(A)** and decreased promoter binding **(B)** in leukemia bone marrow (BM) cells from mice compared to *in vitro* fetal liver (FL) cells, generated using the ClusterProfiler package. The size of each bubble corresponds to the gene count associated with the respective pathway, while the color gradient represents the adjusted p-value of the enriched pathways.

Supplementary Figure 6. Correlation analysis of samples similarity across ACT-seq and ATAC-seq data. (A-B) Jaccard statistic showing similarity between **(A)** ATAC peak-files, **(B)** H3K4me1 ACT-seq peak-files, **(C)** Jaccard statistic between H3K4me3 ACT-seq peak-files and **(D)** Jaccard statistic between MNX1-HA peak-files as determined by bedtools jaccard function. **(E)** Network graph showing the percentage of overlap between the replicates of MNX1 ACT-seq

(nodes). LK1-B: MNX1 BM.1, LK2-B: MNX1 BM.2, LK3-B: MNX1 BM.3, LK4-B: MNX1 BM.4

Supplementary Figure 7. Comparative Analysis of Sample Similarity in MNX1 ACT-seq Data. (A-C) Heatmap displaying MNX1 binding profiles at transcription start sites (TSS) obtained from the refTSS database. Read counts from all MNX1 ACT-seq experiments were extracted within a ±1 kb window around the TSS. Only regions where MNX1 peaks were detected in at least one replicate are shown, while regions lacking MNX1 peaks in all replicates were omitted. The red-to-white gradient represents high-to-low read counts in the respective regions. **(D-E)** Genomic occupancy profiles of ACT-seq signals, highlighting regions with consistently well-defined enrichment peaks across all replicates (right panel) extracted from **(C)** and regions exhibiting dynamic changes in peak enrichment between replicates (left panel) extracted from **(B).**

Supplementary Figure 8. Correlation analysis of MNX1-motifs. Lower half of a correlation matrix depicting the pairwise correlation between each of the top 10 motifs found in the MNX1 ACT-seq peaks of leukemic bone marrow cells from each individual mice and in MNX1 ChIP-seq from insulinoma cells. The first of the two numbers indexing the motifs is the rank of the motif in the used peak set, and the second number denotes which peak set. 1=MNX1 BM1, 2=MNX1 BM2, 3=MNX1 BM3, 4=MNX1 BM4 and Ins=ChIP-seq of MNX1 in insulinoma cells. The correlation score is the average Pearson correlation of all possible pattern matches between two motifs. Clusters highlighted with a thick border are motifs found in all peak sets and the corresponding motif-logo is taken from the MNX1 BM1 peak set.

Supplementary Figure 9. Pathway enrichment analysis for Pbx1 motifs enriched over MNX1 promoters. Bubble plot showing the pathway enrichment analysis for Pbx1 motifs enriched over MNX1 promoters from (upper) ATAC-seq and (lower) H3K4me3 ACT-seq , generated using the ClusterProfiler package. The size of each bubble corresponds to the gene count associated with the respective pathway, while the color gradient represents the adjusted p-value of the enriched pathways.